TRANSPORT THEORY AND STATISTICAL PHYSICS, 14(4), 497-512 (1985)

# The $F_N$-Method in Kinetic Theory: II. Heat Transfer between Parallel Plates

D. Valougeorgis

J. R. Thomas, Jr.

Mechanical Engineering Department
Virginia Polytechnic Institute and State University
Blacksburg, Virginia 24061
USA

## ABSTRACT

The $F_N$ method is used to solve the much-studied problem of heat transfer in a rarefied gas between two parallel plates. The objective is to demonstrate the efficiency of this method for providing solutions of benchmark accuracy to kinetic theory problems in finite media, so that it may be applied with confidence to problems for which more exact methods of analysis do not appear possible.

Singular integral equations for the distribution function are derived and solved by polynomial expansion and collocation. The total heat flux, temperature and density profiles, and the molecular distribution function at various locations between the plates are all computed to high accuracy with relatively low-order approximations.

## I. Introduction

In the previous paper[1] the present authors reported application of the $F_N$ method to two half-space problems of kinetic theory. Very



 0041-1450/85/1404-0497$3.50/0

accurate results were reported based on a relatively simple approximation. In this paper we turn to a problem in a finite medium, that of heat transfer in a gas confined between parallel plates. Our purpose here is to test the $F_N$ method for finite geometry, since in other fields of application of this method, finite geometries have required different forms for the approximate solution. We have chosen a problem which has previously been solved[2,3] by relatively exact methods in order to have a basis of comparison. Our ultimate objective is to solve problems not amenable to such exact treatment but it is important to first develop a background of experience to provide guidelines in such applications and to aid in judging the accuracy to expect of the method.

In Refs. 2 and 3 Thomas et al. formulated this problem and used the method of elementary solutions[4] and half-range orthogonality to provide a solution of benchmark accuracy. We will refer to these papers for the problem formulation and notation. In the present work we rely on the much more tractable full-range orthogonality to develop our approximate solution. It is this reliance on full-range orthogonality alone which makes the $F_N$ method promising for application to more difficult problems.

Referring to Thomas et al.[2,3], we seek the solution of

$$\mu \frac{\partial}{\partial x} \underset{\sim}{\Psi}(x,\mu) + \underset{\sim}{\Psi}(x,\mu) = \frac{1}{\sqrt{\pi}} Q(\mu) \int_{-\infty}^{\infty} \tilde{Q}(\mu') \underset{\sim}{\Psi}(x,\mu') e^{-\mu'^2} d\mu' . \qquad (1)$$

which satisfies the boundary conditions

$$\underset{\sim}{\Psi}(0,\mu) = (1 - \alpha_1) \underset{\sim}{\Psi}(0, -\mu) , \quad \mu > 0 , \qquad (2)$$

and

$$\underset{\sim}{\Psi}(\delta, -\mu) = (1 - \alpha_2)\, \underset{\sim}{\Psi}(\delta,\mu) + \alpha_2\sqrt{\pi} \begin{bmatrix} \mu^2 + B \\ 1 \end{bmatrix}, \quad \mu > 0 . \tag{3}$$

Here $\underset{\sim}{\Psi}(x,\mu)$ is a 2-vector related to perturbations in the density and temperature of the gas[3]:

$$\Delta T(x) = \frac{2}{3\pi} \int_{-\infty}^{\infty} \begin{bmatrix} \mu^2 - 1/2 \\ 1 \end{bmatrix}^T \underset{\sim}{\Psi}(x,\mu)\, e^{-\mu^2}\, d\mu , \tag{4}$$

and

$$\Delta N(x) = \frac{1}{\pi} \int_{-\infty}^{\infty} \begin{bmatrix} 1 \\ 0 \end{bmatrix}^T \underset{\sim}{\Psi}(x,\mu)\, e^{-\mu^2}\, d\mu . \tag{5}$$

We use the superscript T or tilde to denote the transpose operation. Similarly, the normalized heat flux q is related to $\underset{\sim}{\Psi}(x,\mu)$ through[3]

$$q = \frac{Q}{Q_{fm}} = -\frac{\alpha_1 + \alpha_2 - \alpha_1\alpha_2}{\alpha_1\,\alpha_2} \frac{1}{\sqrt{\pi}} \int_{-\infty}^{\infty} \begin{bmatrix} \mu^2 + 1 \\ 1 \end{bmatrix}^T \underset{\sim}{\Psi}(x,\mu)\, \mu\, e^{-\mu^2}\, d\mu. \tag{6}$$

In Eq. (1), $\underset{\sim}{Q}(\mu)$ is a 2 x 2 matrix of polynomials given explicitly elsewhere[3], whereas B in Eq. (3) is a constant to be determined by the condition of mass conservation at the boundary:

$$\begin{bmatrix} 1 \\ 0 \end{bmatrix}^T \int_{-\infty}^{\infty} \underset{\sim}{\Psi}(x,\mu)\, \mu\, e^{-\mu^2}\, d\mu = 0. \tag{7}$$

The boundary conditions (2) and (3) are the Maxwell diffuse-specular conditions with $\alpha_1$ and $\alpha_2$ the accommodation coefficients at the left (x=0) and right (x=δ) surfaces, respectively. In Eq. (6), Q represents the actual heat flux, and $Q_{fm}$ the free-molecular heat flux.

The general solution of this problem is[4]

$$\underset{\sim}{\Psi}(x,\mu) = \sum_{\alpha=1}^{2} A_\alpha \underset{\sim}{\Phi}_\alpha(\mu) + \sum_{\alpha=3}^{4} A_\alpha \underset{\sim}{\Psi}_\alpha(x,\mu) + \sum_{\alpha=1}^{2} \int_{-\infty}^{\infty} A_\alpha(\eta)\, \underset{\sim}{\Phi}_\alpha(\eta,\mu) e^{-x/\eta} d\eta \ . \tag{8}$$

## II. BASIC ANALYSIS

Using full-range orthogonality[4], we derive the singular integral equations

$$\int_{-\infty}^{\infty} \underset{\sim}{\tilde{X}}_\alpha(\mu)\, \underset{\sim}{\Psi}(\delta,\mu)\mu e^{-\mu^2} d\mu - \int_{-\infty}^{\infty} [\underset{\sim}{\tilde{X}}_\alpha(\mu) - \delta\, \underset{\sim}{\tilde{X}}_{\alpha+2}(\mu)]\underset{\sim}{\Psi}(0,\mu)\mu e^{-\mu^2} d\mu = 0, \tag{9}$$

$$\int_{-\infty}^{\infty} \underset{\sim}{\tilde{X}}_{\alpha+2}(\mu)\underset{\sim}{\Psi}(\delta,\mu)\mu e^{-\mu^2} d\mu - \int_{-\infty}^{\infty} \underset{\sim}{\tilde{X}}_{\alpha+2}(\mu)\underset{\sim}{\Psi}(0,\mu)\mu e^{-\mu^2} d\mu = 0, \tag{10}$$

$$\int_{-\infty}^{\infty} \underset{\sim}{\tilde{X}}_\alpha(\eta,\mu)\underset{\sim}{\Psi}(0,\mu)\mu e^{-\mu^2} d\mu - e^{\delta/\eta}\int_{-\infty}^{\infty} \underset{\sim}{\tilde{X}}_\alpha(\eta,\mu)\underset{\sim}{\Psi}(\delta,\mu)\mu e^{-\mu^2} d\mu = 0, \tag{11}$$

and

$$\int_{-\infty}^{\infty} \underset{\sim}{\tilde{X}}_\alpha(-\eta,\mu)\underset{\sim}{\Psi}(0,\mu)\mu e^{-\mu^2} d\mu - e^{-\delta/\eta}\int_{-\infty}^{\infty} \underset{\sim}{\tilde{X}}_\alpha(-\eta,\mu)\underset{\sim}{\Psi}(\delta,\mu)\mu e^{-\mu^2} d\mu = 0, \tag{12}$$

for $\alpha = 1,2$. Here $\underset{\sim}{X}_\alpha(\mu)$, $\underset{\sim}{X}_\alpha(\eta,\mu)$ are the full-range adjoint vectors given explicitly by Kriese et al.[4]

We now introduce the approximations

$$\underset{\sim}{\Psi}(0,-\mu) = \sum_{n=0}^{N} \underset{\sim}{A}_n \mu^n, \quad \mu > 0 \ , \tag{13}$$

and

$$\underset{\sim}{\Psi}(\delta,\mu) = \sum_{n=0}^{N} \underset{\sim}{B}_n \mu^n, \quad \mu > 0 \ . \tag{14}$$

Substituting these approximations into Eqs. (9-12) and utilizing the boundary conditions (2), (3), we find the equations

$$\int_0^\infty [(1-\alpha_1)\underset{\sim}{\chi}_\alpha(-\eta,\mu) - \underset{\sim}{\chi}_\alpha(\eta,\mu)] \sum_{n=0}^{N} \underset{\sim}{A}_n \mu^{n+1} e^{-\mu^2} d\mu$$

$$+ e^{-\delta/\eta} \int_0^\infty [(1-\alpha_2)\underset{\sim}{\chi}_\alpha(\eta,\mu) - \underset{\sim}{\chi}_\alpha(-\eta,\mu)] \sum_{n=0}^{N} \underset{\sim}{B}_n \mu^{n+1} e^{-\mu^2} d\mu$$

$$= -\alpha_2 \sqrt{\pi}\, e^{-\delta/\eta} \int_0^\infty \underset{\sim}{\chi}_\alpha(\eta,\mu) \begin{bmatrix} \mu^2 + B \\ 1 \end{bmatrix} \mu e^{-\mu^2} d\mu, \quad \alpha = 1,2 ; \tag{15}$$

$$\int_0^\infty [(1-\alpha_1)\underset{\sim}{\chi}_\alpha(\eta,\mu) - \underset{\sim}{\chi}_\alpha(-\eta,\mu)] \sum_{n=0}^{N} \underset{\sim}{A}_n \mu^{n+1} e^{-\mu^2} d\mu$$

$$+ e^{\delta/\eta} \int_0^\infty [(1-\alpha_2)\underset{\sim}{\chi}_\alpha(-\eta,\mu) - \underset{\sim}{\chi}_\alpha(\eta,\mu)] \sum_{n=0}^{N} \underset{\sim}{B}_n \mu^{n+1} e^{-\mu^2} d\mu$$

$$= -\alpha_2 \sqrt{\pi}\, e^{\delta/\eta} \int_0^\infty \underset{\sim}{\chi}_\alpha(-\eta,\mu) \begin{bmatrix} \mu^2 + B \\ 1 \end{bmatrix} \mu e^{-\mu^2} d\mu, \quad \alpha = 1,2; \tag{16}$$

$$\int_0^\infty [(2-\alpha_1)\underset{\sim}{\chi}_\alpha(\mu) + \alpha_1 \delta\, \underset{\sim}{\chi}_{\alpha+2}(\mu)] \sum_{n=0}^{N} A_n \mu^{n+1} e^{-\mu^2} d\mu$$

$$- \int_0^\infty (2-\alpha_2)\underset{\sim}{\chi}_\alpha(\mu) \sum_{n=0}^{N} \underset{\sim}{B}_n \mu^{n+1} e^{-\mu^2} d\mu$$

$$= \alpha_2 \sqrt{\pi} \int_0^\infty \underset{\sim}{\chi}_\alpha(\mu) \begin{bmatrix} \mu^2 + B \\ 1 \end{bmatrix} \mu e^{-\mu^2} d\mu, \quad \alpha = 1,2; \tag{17}$$

**and**

$$\alpha_1 \int_0^\infty \underset{\sim}{\chi}_\alpha(\mu) \sum_{n=0}^{N} \underset{\sim}{A}_n \mu^{n+1} e^{-\mu^2} d\mu + \alpha_2 \int_0^\infty \underset{\sim}{\chi}_\alpha(\mu) \sum_{n=0}^{N} \underset{\sim}{B}_n \mu^{n+1} e^{-\mu^2} d\mu$$

$$= \alpha_2 \sqrt{\pi} \int_0^\infty \underset{\sim}{\chi}_\alpha(\mu) \begin{bmatrix} \mu^2 + B \\ 1 \end{bmatrix} \mu e^{-\mu^2} d\mu, \quad \alpha = 3,4. \tag{18}$$

When the eigenvectors $\underset{\sim}{X}_\alpha(\mu)$ and $\underset{\sim}{X}_\alpha(\eta,\mu)$ are introduced explicitly into Eqs. (12-15), it is found that all integrals can be reduced to combinations of the basic integral

$$I(\xi) = \int_0^\infty \frac{e^{-\xi^2} d\mu}{\mu + \xi} \tag{19}$$

which we evaluate numerically using Gaussian quadrature. Since each of the coefficients $\underset{\sim}{A}_n$ and $\underset{\sim}{B}_n$ have two components, we have a total of 4N + 4 unknowns; evaluating Eqs. (15) and (16) at N discrete values of $\xi \in (0,\infty)$ leads to a system of 4N + 4 linear algebraic equations when Eqs. (17) and (18) are included. These equations are too lengthy to repeat here and are given explicitly elsewhere[5]. The condition of mass conservation (7) can be used to express the constant B of Eq. (3) in terms of the unknown $F_N$ coefficients $\underset{\sim}{B}_n$:

$$B = -1 + \frac{2}{\sqrt{\pi}} \begin{bmatrix} 1 \\ 0 \end{bmatrix}^T \sum_{n=0}^{N} \underset{\sim}{B}_n \int_0^\infty \mu^{n+1} e^{-\mu^2} d\mu \,. \tag{20}$$

Once the system of linear equations is solved, the heat flux and the temperature and density profiles can readily be determined. Inserting the general solution (8) into Eq. (6) yields

$$q = -\frac{\alpha_1 + \alpha_2 - \alpha_1\alpha_2}{\alpha_1\,\alpha_2} \frac{5}{8}\sqrt{\frac{2}{3}}\, A_3, \tag{21}$$

where

$$A_3 = \int_{-\infty}^{\infty} \underset{\sim}{\tilde{X}}_3(\mu)\, \underset{\sim}{\Psi}(0,\mu)\, \mu^{n+1} e^{-\mu^2} d\mu, \tag{22}$$

which can be evaluated in terms of the $F_N$ coefficients as

$$A_3 = - \alpha_1 \int_0^\infty \underset{\sim}{\chi}_3(\mu) \sum_{n=0}^{N} \underset{\sim}{A}_n \mu^{n+1} e^{-\mu^2} d\mu . \qquad (23)$$

The temperature and density profiles may similarly be expressed[8] as

$$\Delta T(x) = \sqrt{\frac{2}{3\pi}} (A_1 - A_3 x) + \frac{1}{\pi} \int_0^\infty [ A_1(\eta) e^{-x/\eta} + A_1(-\eta) e^{x/\eta} ] e^{-\eta^2} d\eta, \qquad (24)$$

and

$$\Delta N(x) = \frac{1}{\sqrt{\pi}} (A_2 - A_4 x) + \frac{1}{\pi} \int_0^\infty [ A_2(\eta) e^{-x/\eta} + A_2(-\eta) e^{x/\eta} ] e^{-\eta^2} d\eta, \qquad (25)$$

where the $A_m$ and $A_m(\eta)$ can be determined through expressions analogous to Eq. (22).

## III. Position-Dependent Quantities

We prefer to use a different approach[6,7] which gives the temperature and density profiles directly through Eqs. (4) and (5), as well as the molecular distribution function.

Through a procedure analogous to that used in deriving Eqs. (9-12), we find for any x in $[0,\delta]$

$$\int_{-\infty}^{\infty} \underset{\sim}{\chi}_\alpha(\eta,\mu) \underset{\sim}{\Psi}(0,\mu) \mu e^{-\mu^2} d\mu - e^{x/\eta} \int_{-\infty}^{\infty} \underset{\sim}{\chi}_\alpha(\eta,\mu) \underset{\sim}{\Psi}(x,\mu) \mu e^{-\mu^2} d\mu = 0, \qquad (26)$$

$$\int_{-\infty}^{\infty} \underset{\sim}{\chi}_\alpha(-\eta,\mu) \underset{\sim}{\Psi}(0,\mu) \mu e^{-\mu^2} d\mu - e^{-x/\eta} \int_{-\infty}^{\infty} \underset{\sim}{\chi}_\alpha(-\eta,\mu) \underset{\sim}{\Psi}(x,\mu) \mu e^{-\mu^2} d\mu = 0, \qquad (27)$$

$$\int_{-\infty}^{\infty} \underset{\sim}{\chi}_\alpha(\mu) \underset{\sim}{\Psi}(x,\mu) \mu e^{-\mu^2} d\mu - \int_{-\infty}^{\infty} [\underset{\sim}{\chi}_\alpha(\mu) - \mu \underset{\sim}{\chi}_{\alpha+2}(\mu)] \underset{\sim}{\Psi}(0,\mu) \mu e^{-\mu^2} d\mu = 0, \qquad (28)$$

for $\alpha = 1, 2$, and

$$\int_{-\infty}^{\infty} \underset{\sim}{\chi}_{\alpha}(\mu)\underset{\sim}{\Psi}(x,\mu)\mu e^{-\mu^2} d\mu - \int_{-\infty}^{\infty} \underset{\sim}{\chi}_{\alpha}(\mu)\underset{\sim}{\Psi}(0,\mu)\ \mu e^{-\mu^2} d\mu = 0, \tag{29}$$

for $\alpha = 3, 4$. We approximate $\underset{\sim}{\Psi}(0,\mu)$ as in Eq. (13), and use

$$\underset{\sim}{\Psi}(x,\mu) = \sum_{m=0}^{N} \underset{\sim}{F}_m(x)\ \mu^m, \quad \mu > 0\ , \tag{30}$$

and

$$\underset{\sim}{\Psi}(x,-\mu) = \sum_{m=0}^{N} \underset{\sim}{G}_m(x)\ \mu^m, \quad \mu > 0\ , \tag{31}$$

in Eqs. (26-29) to obtain the equations

$$\sum_{m=0}^{N} \int_{0}^{\infty} \underset{\sim}{\chi}_{\alpha}(\eta,-\mu)\ \mu^{m+1} e^{-\mu^2} d\mu\ \underset{\sim}{F}_m(x)$$

$$- \sum_{m=0}^{N} \int_{0}^{\infty} \underset{\sim}{\chi}_{\alpha}(\eta,\mu)\ \mu^{m+1} e^{-\mu^2} d\mu\ \underset{\sim}{G}_m(x)$$

$$= e^{x/\eta} \sum_{m=0}^{N} \int_{0}^{\infty} [(1 - \alpha_1)\underset{\sim}{\chi}_{\alpha}(\eta,-\mu) - \underset{\sim}{\chi}_{\alpha}(\eta,\mu)]\mu^{m+1} e^{-\mu^2} d\mu\ \underset{\sim}{A}_m, \tag{32}$$

$$\sum_{m=0}^{N} \int_{0}^{\infty} \underset{\sim}{\chi}_{\alpha}(\eta,\mu)\ \mu^{m+1} e^{-\mu^2} d\mu\ \underset{\sim}{F}_m(x)$$

$$- \sum_{m=0}^{N} \int_{0}^{\infty} \underset{\sim}{\chi}_{\alpha}(\eta,-\mu)\ \mu^{m+1} e^{-\mu^2} d\mu\ \underset{\sim}{G}_m(x)$$

$$= - e^{-x/\eta} \sum_{m=0}^{N} \int_{0}^{\infty} [(1-\alpha_1)\underset{\sim}{\chi}_{\alpha}(\eta,\mu) - \underset{\sim}{\chi}_{\alpha}(\eta,-\mu)]\mu^{m+1} e^{-\mu^2} d\mu\ \underset{\sim}{A}_m, \tag{33}$$

$$\sum_{m=0}^{N} \int_{0}^{\infty} \underset{\sim}{\chi}_{\alpha}(\mu)\mu^{m+1} e^{-\mu^2} d\mu\ [\underset{\sim}{F}_m(x) + \underset{\sim}{G}_m(x)]$$

$$= \sum_{m=0}^{N} \int_0^\infty [(2 - \alpha_1)\underset{\sim}{\chi}_\alpha(\mu) + \mu\, \alpha_1\, \underset{\sim}{\chi}_{\alpha+2}(\mu)]\, \mu^{m+1} e^{-\mu^2} d\mu\, \underset{\sim}{A}_m, \tag{34}$$

for $\alpha = 1, 2$, and

$$\sum_{m=0}^{N} \int_0^\infty \underset{\sim}{\chi}_\alpha(\mu)\, \mu^{m+1} e^{-\mu^2} d\mu\, [\underset{\sim}{F}_m(x) - \underset{\sim}{G}_m(x)]$$

$$= \alpha_1 \sum_{m=0}^{N} \int_0^\infty \underset{\sim}{\chi}_\alpha(\mu)\, \mu^{m+1} e^{-\mu^2} d\mu\, \underset{\sim}{A}_m, \tag{35}$$

for $\alpha = 3, 4$.

The integrals involved in Eqs. (32-35) may be reduced to exactly those appearing in Eqs. (15-18), so that no new quantities have to be computed. We evaluate Eqs. (32) and (33) at N values of $\eta \in (0, \infty)$ to achieve, along with Eqs. (33) and (34), a total of 4N + 4 equations for the 4N + 4 unknowns $\underset{\sim}{F}_m(x)$ and $\underset{\sim}{G}_m(x)$. This system of equations is then solved for $F_m(x)$ and $G_m(x)$ at each value of x of interest. With these quantities known, the temperature and density profiles and the heat flux follow immediately from Eqs. (4-6), and (30), (31). The matrix of coefficients in Eqs. (32-35) is independent of x, so that the solution for all x can be accomplished with only one matrix inversion.

This approach allows us to calculate in addition the "reduced" distribution function

$$F(x, \xi_1) \triangleq \int_{-\infty}^{\infty} \int_{-\infty}^{\infty} f(x, \underset{\sim}{\xi})\, d\xi_2 d\xi_3, \tag{36}$$

where $f(x, \underset{\sim}{\xi})$ is the molecular distribution function at location x and velocity $\underset{\sim}{\xi} = (\xi_1, \xi_2, \xi_3)$. We find

$$F(x,\xi_1) = \frac{\rho_1}{(2\pi RT_1)^{1/2}}\left[1 + \frac{\Delta T}{\sqrt{\pi}\,T_1}\begin{bmatrix}1\\0\end{bmatrix}^T \underset{\sim}{\Psi}(x,\xi_1)\right] e^{-\xi_1^2/2RT_1}, \qquad (37)$$

where

$$\Delta T = T_2 - T_1 .$$

## IV. Numerical Results

In order to solve for the coefficients in the $F_N$ expansion, we must first choose a set of collocation points $\{\eta_j\} \in [0,\infty)$, $j = 0,1,\ldots N$, at which to evaluate Eqs. (15-18) and (32-35). In obtaining the numerical results to follow, we used the positive zeros of the Hermite polynomials of degree 2N.

In Table I we illustrate the convergence of the $F_N$ method by tabulating values of the heat flux q as computed from Eqs. (6) or (21) vs. the order of approximation N. We also show the "exact" results based on half-range analysis[3]. It is seen that a low-order approximation gives results correct to five or six significant figures for inverse Knudsen numbers $\delta < 0.01$ and $\delta > 0.10$. For $0.01 \leq \delta \leq 1.0$, four significant figures seem to be the limit for simple polynomial approximations of the form shown in Eqs. (13) and (14).

We tabulate converged values of the heat flux by comparison to Ref. 3 in Table II for several different values of the accommodation coefficients, and for $\delta = 5.0$. Five-significant-figure accuracy was obtained for all values of $\alpha$ tested.

Temperature and density profiles are shown in Tables III and IV, as computed from Eqs. (4) and (5) using the x-dependent approximations of Eqs. (30) and (31) for representative values of $\alpha$ and $\delta$. For most

Table I. Convergence of the Normalized Heat Flux for $\alpha_1 = 0.7$ and $\alpha_2 = 0.3$

| $\delta$ | $F_4$ | $F_8$ | $F_{12}$ | $F_{16}$ | $F_{18}$ | $F_{20}$ | $F_{22}$ | $F_{24}$ | Converged Results | Exact |
|---|---|---|---|---|---|---|---|---|---|---|
| 0.0 | 1.000000 | 1.000000 | | | | | | | 1.000000 | 1.000000 |
| 0.001 | 0.999815 | 0.999810 | 0.999807 | 0.999806 | 0.999805 | 0.999804 | 0.999804 | 0.999803 | 0.999803 | 0.999794 |
| 0.01 | 0.998157 | 0.998105 | 0.998080 | 0.998064 | 0.998057 | 0.998053 | 0.998049 | 0.998046 | 0.99804 | 0.997966 |
| 0.5 | 0.921005 | 0.920651 | 0.920647 | 0.920696 | 0.920723 | 0.920745 | 0.920769 | 0.920778 | 0.92078 | 0.920840 |
| 1.0 | 0.861922 | 0.862139 | 0.682257 | 0.862297 | 0.862302 | 0.862297 | 0.862291 | 0.862289 | 0.86229 | 0.862238 |
| 2.0 | 0.772297 | 0.772374 | 0.772335 | 0.772303 | 0.772293 | 0.772293 | | | 0.772293 | 0.772293 |
| 3.0 | 0.703051 | 0.703017 | 0.702982 | 0.702977 | 0.702979 | 0.702979 | | | 0.702979 | 0.702979 |
| 4.0 | 0.646558 | 0.646515 | 0.646503 | 0.646506 | 0.646507 | 0.646506 | 0.646505 | 0.646505 | 0.646505 | 0.646500 |
| 5.0 | 0.599104 | 0.599068 | 0.599065 | 0.599065 | 0.599064 | 0.599063 | 0.599062 | 0.599062 | 0.599062 | 0.599058 |
| 7.0 | 0.523124 | 0.523010 | 0.523097 | 0.523094 | 0.523093 | 0.523093 | 0.523092 | 0.523092 | 0.523092 | 0.523090 |
| 10.0 | 0.439993 | 0.439978 | 0.439975 | 0.439973 | 0.439972 | 0.439972 | 0.439971 | 0.439971 | 0.439971 | 0.439970 |
| 100.0 | 0.0765027 | 0.0765023 | 0.0765022 | 0.0765022 | 0.0765022 | 0.0765021 | 0.0765021 | | 0.0765021 | 0.0765021 |

Table II. Normalized Heat Flux for $\delta = 5.0$.

| $\alpha_1$ | $\alpha_2$ | $F_{24}$ | Exact [3] |
|---|---|---|---|
| 0.7 | 0.9 | 0.384792 | 0.384790 |
| 0.7 | 0.7 | 0.428231 | 0.428228 |
| 0.7 | 0.5 | 0.492920 | 0.492918 |
| 0.7 | 0.3 | 0.599062 | 0.599058 |
| 0.7 | 0.1 | 0.804266 | 0.804263 |
| 1.0 | 0.9 | 0.313373 | 0.313371 |
| 1.0 | 0.8 | 0.338420 | 0.338418 |
| 1.0 | 0.7 | 0.368048 | 0.368046 |
| 1.0 | 0.6 | 0.403647 | 0.403645 |
| 1.0 | 0.5 | 0.447229 | 0.447227 |

Table III. Density and Temperature Profiles for $\delta = 2.0$, $\alpha_1 = 0.7$, $\alpha_2 = 0.3$

| x | Temperature | | Density | |
|---|---|---|---|---|
| | $F_{24}$ | Exact | $F_{24}$ | Exact |
| 0.0 | 0.162708 | 0.162708 | -0.077030 | -0.077013 |
| 0.1 | 0.201816 | 0.201815 | -0.112758 | -0.112759 |
| 0.2 | 0.230009 | 0.230008 | -0.138712 | -0.138712 |
| 0.3 | 0.255699 | 0.255698 | -0.162572 | -0.162571 |
| 0.4 | 0.280355 | 0.280354 | -0.185587 | -0.185586 |
| 0.5 | 0.304688 | 0.304687 | -0.208338 | -0.208337 |
| 0.6 | 0.329226 | 0.329224 | -0.231246 | -0.231245 |
| 0.7 | 0.354539 | 0.354537 | -0.254767 | -0.254767 |
| 0.8 | 0.381505 | 0.381502 | -0.279627 | -0.279626 |
| 0.9 | 0.412078 | 0.412076 | -0.307500 | -0.307498 |
| 1.0 | 0.457969 | 0.457966 | -0.349100 | -0.349189 |

Table IV. Density and Temperature Profiles for $\delta = 5.0$, $\alpha_1 = 1.0$, $\alpha_2 = 0.5$

| x | Temperature | | Density | |
|---|---|---|---|---|
| | $F_{24}$ | Exact | $F_{24}$ | Exact |
| 0.0 | 0.086631 | 0.086636 | -0.040202 | -0.040212 |
| 0.1 | 0.162129 | 0.162130 | -0.111004 | -0.111008 |
| 0.2 | 0.220969 | 0.220970 | -0.167637 | -0.167640 |
| 0.3 | 0.276591 | 0.276591 | -0.221814 | -0.221817 |
| 0.4 | 0.330985 | 0.330985 | -0.275087 | -0.275089 |
| 0.5 | 0.385032 | 0.385032 | -0.328106 | -0.328108 |
| 0.6 | 0.439368 | 0.439367 | -0.381329 | -0.381331 |
| 0.7 | 0.494712 | 0.494711 | -0.435279 | -0.435280 |
| 0.8 | 0.552291 | 0.552289 | -0.490869 | -0.490870 |
| 0.9 | 0.615159 | 0.615156 | -0.550494 | -0.550497 |
| 1.0 | 0.705115 | 0.705149 | -0.633270 | -0.633331 |

cases five or six significant figures are correct. These profiles were computed in two different ways: through Eqs. (24) and (25) with the expansion coefficients $A_\alpha$, $\alpha = 1,\ldots,4$ and $A_\alpha(\eta)$, $\alpha = 1,2$ computed from the $F_N$ coefficients as in Eq. (23), and directly through Eqs. (4) and (5) using the x-dependent $F_N$ solutions for the expansion coefficients given by Eqs. (30) and (31). Agreement to at least 5 significant figures was obtained between these two different methods. A similar comparision for two different computations of the heat flux through Eqs. (21) and (23), or Eq. (6) using Eqs. (30) and (31) yielded agreement up to 10 significant figures.

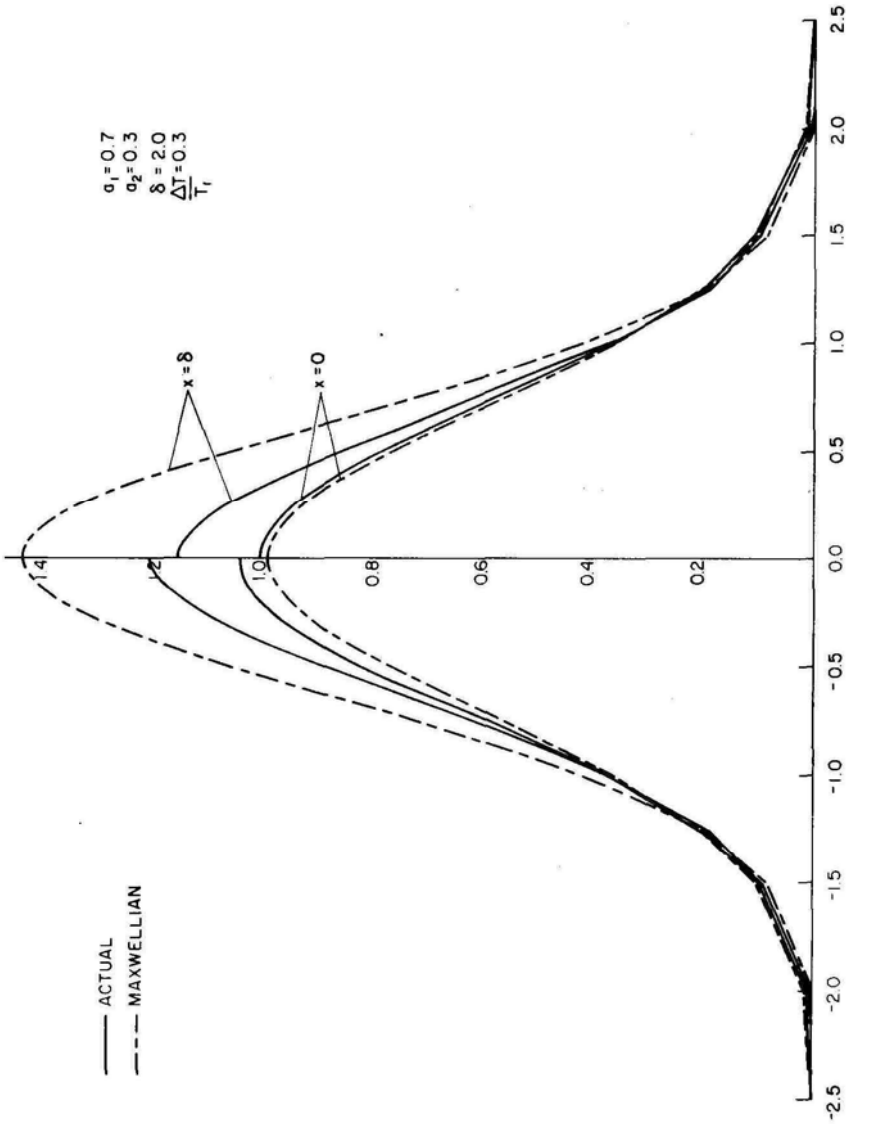


Fig. 1. Reduced distribution function $F(x,\xi_1)$, Eq. (37) vs $\xi_1 = \frac{c_1}{\sqrt{2RT_1}}$

Finally, in Fig. I we show the reduced distribution function of Eq. (37) at x=0 and x=δ. We also show the local Maxwellian distribution at the same locations for comparison. Although the increased departure from equilibrium at the right boundary x = δ is evident, the perturbation in the distribution function is still small enough to justify a linear analysis. The distribution function can only be obtained through the position-dependent approximations (30) and (31).

## Conclusions

We have demonstrated that the $F_N$ method is a viable solution technique for kinetic theory problems in finite media, yielding results of benchmark accuracy for the full Knudsen number range of interest. However, for media of thickness 0.01 to 1.0 mean-free-paths the accuracy does fall to four significant figures. In addition, we have shown that it is possible to compute space-dependent quantities to high accuracy, including the molecular distribution function itself. Study of the distribution function can often be very useful in understanding the physics of more complex kinetic theory problems, such as those involving condensation-evaporation processes[9]. The method should be quite useful in solving problems for which exact analysis is not possible.

## Acknowledgement

The authors are grateful to Professor C. E. Siewert for several helpful suggestions. This work was supported in part by the National Science Foundation under grant CPE-8107473.

## References

[1] J. R. Thomas and D. Valougeorgis, Transp. Th. Stat. Phys. (this issue).

[2] J. R. Thomas, Jr., T. S. Chang, and C. E. Siewert, Phys. Fluids 16, 2116 (1973).

[3] J. R. Thomas, Jr., in: Rarefied Gas Dynamics, Sam S. Fisher, ed., AIAA Progress in Aeronautics and Astronautics 74, 363 (1981).

[4] J. T. Kriese, T. S. Chang, and C. E. Siewert, Int. J. Engng. Sci. 12, 441 (1974).

[5] D. Valougeorgis, Ph.D. Dissertation, Virginia Polytechnic Institute and State University, Blacksburg, Virginia (1985).

[6] C. Devaux, C. E. Siewert, and Y. L. Yuan, Astrophys. J. 253, 773 (1982).

[7] R. D. M. Garcia and C. E. Siewert, Nucl. Sci. Eng. 81, 474 (1982).

[8] J. R. Thomas, Jr., Ph.D. Dissertation, North Carolina State University, Raleigh, North Carolina (1973).

[9] C. E. Siewert and J. R. Thomas, Jr., Z. angew Math. Phys. 33, 202 (1982).

Received: January 31, 1985
Revised: May 21, 1985